

Atomic Energy of Canada Limited

CANDU-BLW EXPERIMENTS IN ZED-2

PART II: BOOSTER ROD EXPERIMENTS

by

R. E. KAY

Chalk River, Ontario

March 1967

AECL-2689

CANDU-BLW EXPERIMENTS IN ZED-2
PART II: BOOSTER ROD EXPERIMENTS

by
R.E. KAY

ABSTRACT

Experiments have been performed in a simulated CANDU-BLW lattice in ZED-2 to determine the perturbing effect of a mock-up BLW booster rod on the surrounding lattice, the neutron density distribution within the booster and its reactivity effect.

Experiments were performed with the booster vertical along the axis of the lattice, and horizontal across a diameter of the lattice near the position of maximum axial flux.

The maximum observed neutron density perturbation was $\sim + 55\%$ at a distance ~ 20 cm from the booster.

Reactivity measurements in terms of changes in lattice critical height were made relative to a standard absorber.

Simplified perturbation theory calculations were performed to compare with the measured relative reactivity effects.

Chalk River, Ontario

March, 1967

AECL-2689

CONTENTS

	<u>Page</u>
I. INTRODUCTION	1
II. FUEL AND LATTICE	2
III. EXPERIMENTS	5
1. Macroscopic Neutron Density Measurements	5
2. Detailed Neutron Density Measurements at Booster Rod	12
3. Neutron Spectrum Measurements	12
4. Reactivity Measurements	13
IV. RESULTS AND DISCUSSION	14
1. Lattice Neutron Density Perturbations	14
2. Neutron Density Measurements at Booster Rod	25
a) General	25
b) Average Neutron Density in Booster Rod	29
3. Reactivity Measurements	30
V. REACTIVITY MEASUREMENTS: A COMPARISON WITH CALCULATION	31
VI. STATISTICAL WEIGHT THEORY APPLIED TO THE ROTATION OF THE BOOSTER ROD	35
VII. CONCLUSIONS	36
ACKNOWLEDGEMENTS	38
REFERENCES	39
APPENDIX A. Detailed Neutron Density Measurements in a Lattice Cell; 28 Rod UO ₂ Fuel, H ₂ O Coolant, 11" square lattice pitch.	
APPENDIX B. 'Blackness' Calculation of Neutron Density in ²³⁵ U Fuel.	

FIGURES

CAPTION

	<u>Page</u>
1. Cross Section through 28 Rod Fuel Assembly	3
2. BLW (AT) Lattice Arrangement in ZED-2	4
3. ZEEP Fuel Rod and 7-Rod UO ₂ Fuel Assembly	4
4. Details of Booster Rod and Suspension	6
5. BLW Booster and Support Tube	7
6. BLW Booster Dismantled	7
7. BLW Reference Lattice Arrangement in ZED-2	9
8. BLW Booster Horizontal in ZED-2	10
9. BLW Booster Vertical in ZED-2	11
10. Radial Normalized Neutron Density Distributions in Unperturbed Lattice: Foils in Thimbles	20
11. Radial Normalized Neutron Density Distributions in Unperturbed and Perturbed Lattices	20
12. Axial Relative Total Neutron Density Distribution; Thimble E	21
13. Axial Relative Total Neutron Density Distributions; Foils on North Side of Calandria Tube of F1	21
14. Plot of $F(r,z)$ against Radius; Foils in Thimbles, North-South Direction: Booster Rod Horizontal	22
15. Plot of $F(r,z)$ for Foils in Thimbles and on Calandria Tube in East-West Direction: Booster Rod Horizontal	22
16. Plot of $F(r,z)$ against Distance from Booster for Foils in a North-South Diametral Plane; Booster Rod Horizontal	23
17. Axial Flux Perturbation Factors; Booster Rod Horizontal	23
18. Axial Flux Perturbation Factors; Booster Rod Vertical	24
19. $F(r,z)$ against Radius at 105 cm elevation; Booster Rod Vertical	24
20. Plot of $F(r,z)$ for Foils along Center Line of Horizontal Booster Rod	28
21. Relative Activity Distribution, Rod #1; Booster Rod Horizontal	28

FIGURES (contd)

CAPTION

Appendix A

A1 Relative Manganese Activity Distributions in
Moderator

TABLES

CAPTION

	<u>Page</u>
1. Summary of $r\sqrt{T_n/T_o}$ Values	15
2. Normalized Total Neutron Densities - BLW(AT) Lattice Unperturbed	16
3. Normalized Total Neutron Densities - BLW Booster Horizontal	17
4. Normalized Total Neutron Densities - BLW Booster Vertical	18
5. Flux Perturbation Factors $F(r,z)$ - BLW Booster Horizontal	26
6. Flux Perturbation Factors $F(r,z)$ - BLW Booster Vertical	26
7. Summary of Least Squares Fits to Axial Activity Distributions	27
8. Measurements at Booster Rod	27
9. Lattice Reactivity Data	32
<u>Appendix A</u>	
A1 Relative Total Neutron Density Measurements	

I. INTRODUCTION

This report is the second⁽¹⁾ of a series describing experiments performed in the heavy-water-moderated critical facility ZED-2⁽²⁾ to investigate specific problems relating to the proposed CANDU-BLW reactor⁽³⁾.

In the BLW reactor excess reactivity is required to override ^{135}Xe poison so that the reactor may be started up within 40 minutes of a shutdown and to overcome the effect of the increase in average coolant density (void collapse) which accompanies shutdown. This excess reactivity will be provided by booster rods, highly enriched in ^{235}U , which can be inserted into the lattice interstitially and perpendicular to the fuel channels. These boosters are cooled by heavy water and have a ^{235}U concentration of ~ 5.2 g/cm length.

The strong neutron absorption by the booster rod and its action as a large source of fast neutrons produce large neutron density perturbations about the booster. To prevent overheating in the booster or adjacent fuel channels the magnitude of these perturbations must be known. Further, for control purposes it is essential to know the reactivity worth of the booster rods.

The experiments described here investigate the reactivity effects and flux perturbations on the surrounding lattice due to a booster rod having a ^{235}U content comparable to that of the prototype booster, in a mock-up CANDU-BLW lattice in ZED-2.

The results obtained in these experiments, although not directly applicable to the situation in the power reactor, due to differences in the lattice composition and size and the booster rod construction, do form a standard set of results with which to compare methods of calculation.

II. FUEL AND LATTICE

Because prototype BLW fuel was not available the experiments were performed using a mock-up lattice which approximated in fuel, coolant and moderator absorption areas to that proposed for the prototype BLW reactor. This mock-up lattice was composed of 52, 28-rod UO_2 fuel assemblies arranged in ZED-2 in an open centered square lattice of spacing 27.94 cm (11 in.). Details of the 28-rod UO_2 fuel assemblies are given in Figure 1 and Reference 4. Each fuel rod consists of natural uranium oxide fuel pellets (1.42cm dia., density 10.45 g/cm³) contained in Zircaloy-2 sheaths (1.43cm ID, 0.045 cm wall). Four, eight and sixteen of these rods 49.7 cm long (fuel length 47.7 cm), are located by end plates on three circles of diameters 2.326 cm, 5.304 cm and 8.412 cm respectively, to form a fuel bundle. A fuel assembly consists of five of these bundles within aluminum pressure (ID 10.19 cm, OD 10.78 cm) and calandria (ID 12.46 cm, OD 12.74 cm) tubes.

During operation, the coolant in the BLW reactor will be a mixture of boiling light water and up to 33% steam⁽³⁾; in the experiments described here the coolant was room temperature light water.

Such a lattice has a low reactivity⁽¹⁾ ($B^2 \approx 1.16 \text{ m}^{-2}$) and a 'driver' region was required to achieve a critical system in ZED-2. Figure 2 illustrates the arrangement used. The driver region was composed of 119 or 120 (see Sect. III-4) ZEEP natural uranium metal rods 3.257 cm (1.282") dia. at a pitch of 13.97 cm (5½") placed in an annulus around the BLW fuel zone. [Note: the separation between the last two rows of ZEEP rods on the North side of the reactor was 8.10 cm (3-3/16"); in the neutron density perturbation measurements one ZEEP rod was removed from the centre of the last row on the South side of the core (see Sect. III-4)]. Between

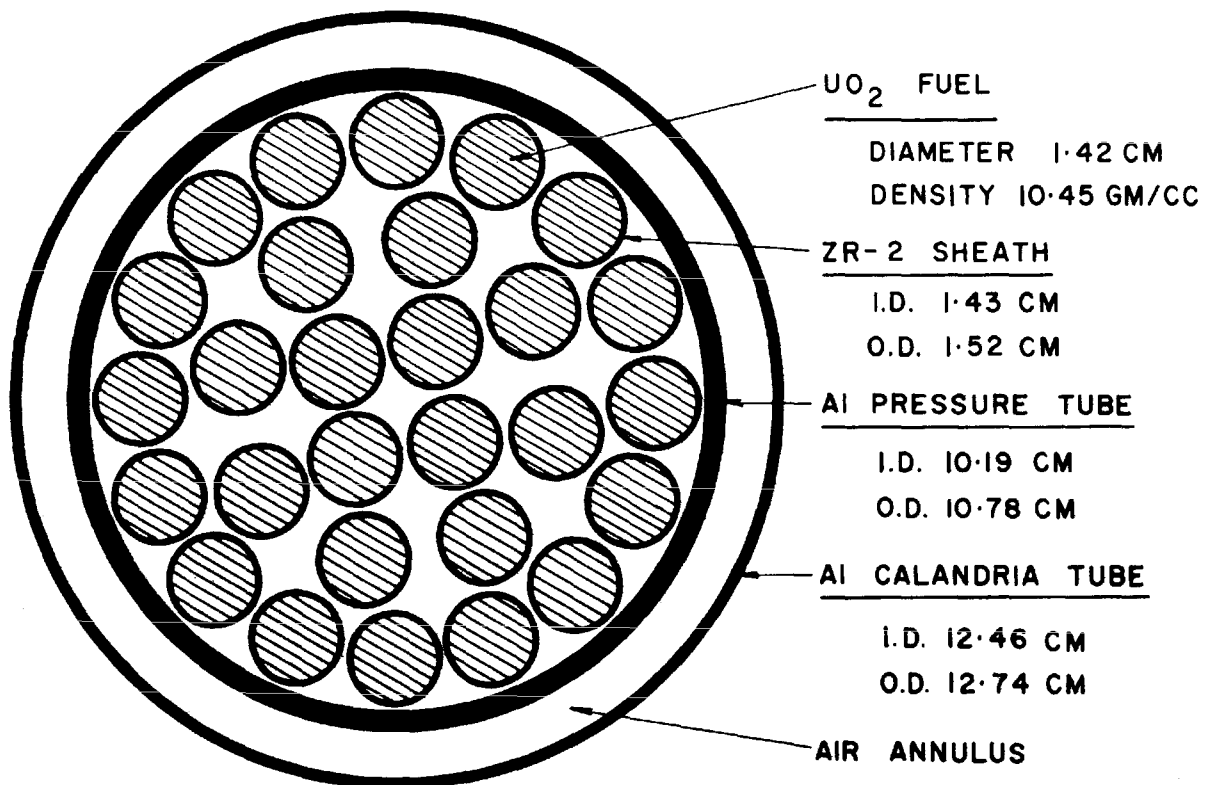


Fig. 1 Cross section through 28 rod fuel assembly

- 28 ROD BUNDLE
- 7 ROD BUNDLE
- ZEEP FUEL ASSEMBLY

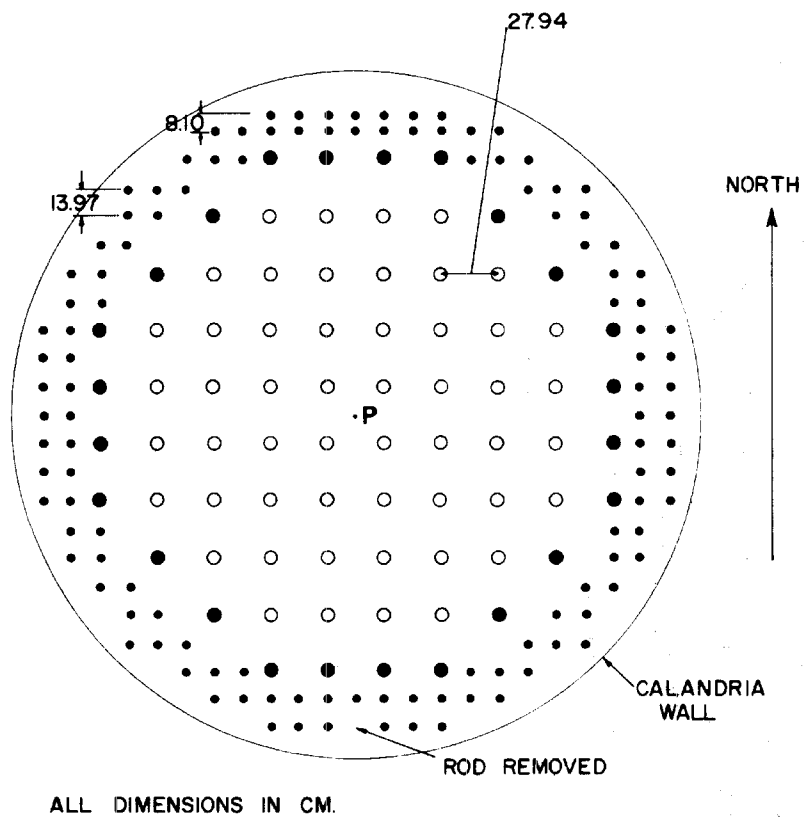


Fig. 2 BLW (AT) lattice arrangement in ZED-2

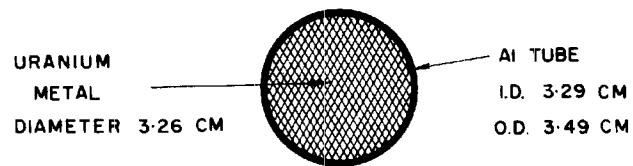


Fig. 3(a) ZEEP fuel rod

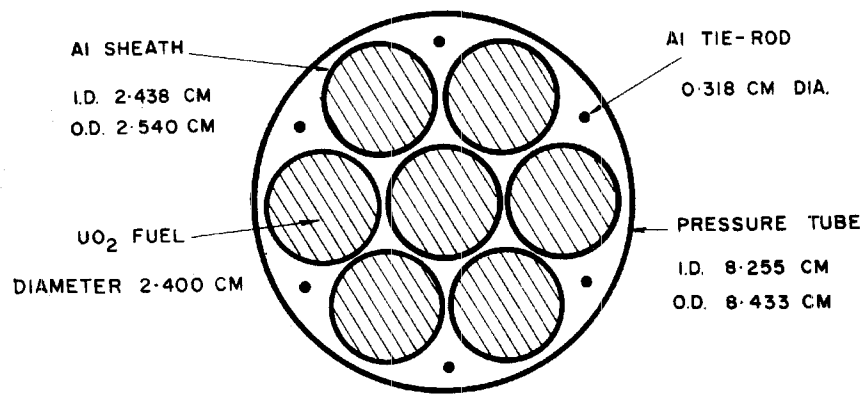


Fig. 3(b) 7-element UO₂ fuel assembly

the driver and BLW zones was a buffer region of 24 air-cooled 7-rod natural uranium oxide fuel assemblies. This buffer zone helped match the spectrum differences at the driver-BLW zone interface. Details of the ZEEP and 7-rod UO_2 fuel assemblies are given in References 5 and 6 and Figure 3.

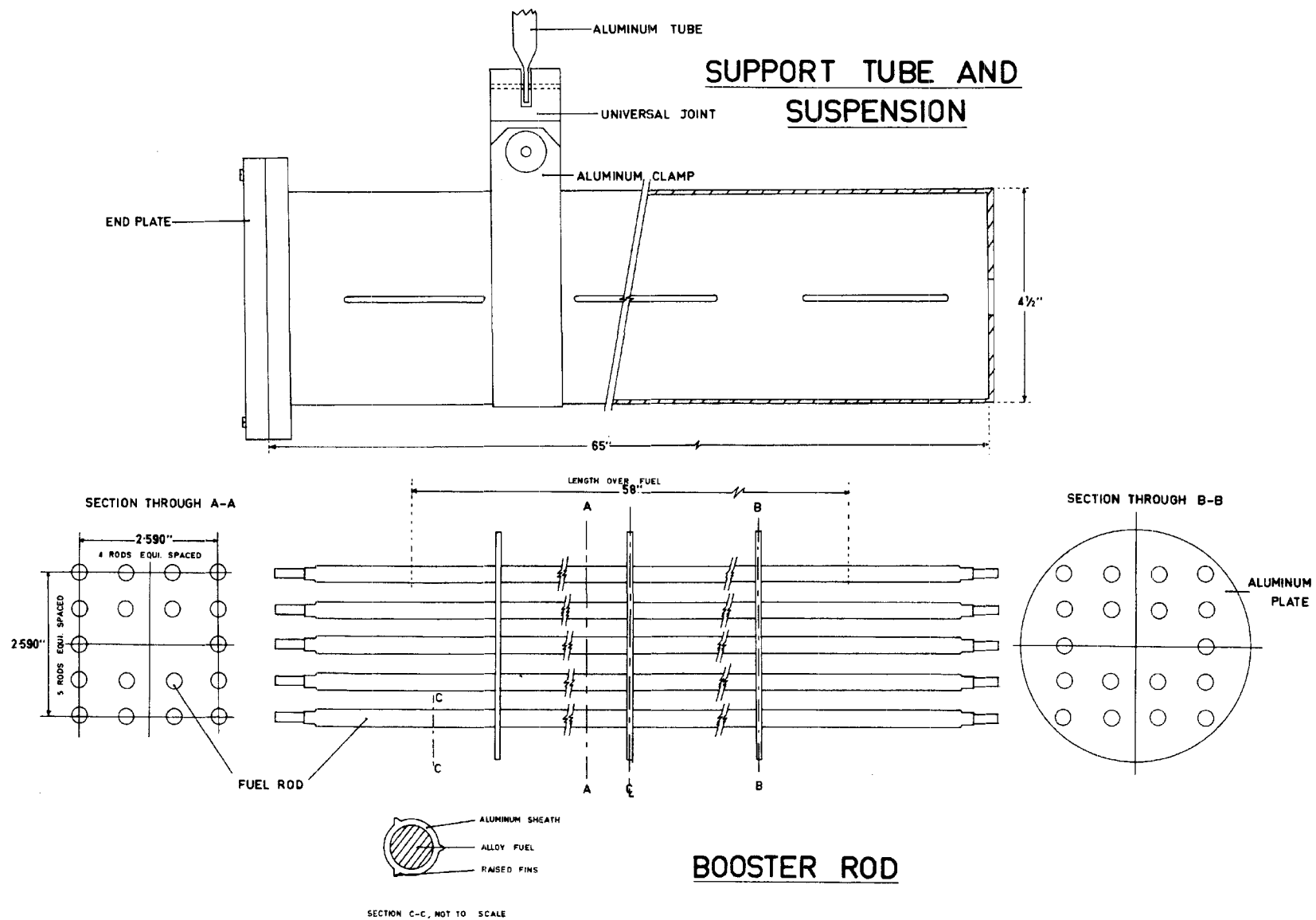
The booster rod simulated in length and ^{235}U content per unit length a booster rod proposed for the BLW reactor. Figures 4, 5 and 6 illustrate the simulated booster and the method of suspension in ZED-2. The booster consists of eighteen $\frac{1}{4}$ " diameter rods of an alloy of 28 w/o uranium (enriched to 93 w/o ^{235}U) and superpure aluminum, sheathed in Alcan 2S aluminum. Figure 4 illustrates the arrangement of the 18 fuel rods; the length over the fuel is 147 cm (58"), the total fuel content of the booster 775 g ^{235}U . To facilitate the attachment of foils to the booster it was arranged to be able to split the booster in half longitudinally; this is done in Figure 6.

For safety in suspending the booster, it was contained in a $4\frac{1}{2}$ " OD aluminum (Alcan 6061) tube of $\frac{1}{16}$ " wall, fitted with end plates (see Figure 4). The booster rod in the support tube was suspended from the beams supporting the fuel assemblies. The horizontal suspension consisted of two aluminum clamps around the support tube connected via universal joints to $\frac{1}{2}$ " OD, 0.047" wall aluminum tubes (see Figures 4, 5 and 6). For vertical suspension a single $3/8$ " OD, $\frac{1}{16}$ " wall aluminum tube was attached to the end plate of the suspension tube. Free access of the D_2O moderator was ensured by holes in the end plates and the walls of the containing tube.

III. EXPERIMENTS

1. Macroscopic Neutron Density Measurements

Experiments were performed to compare the neutron density distributions at typical lattice positions when no perturbation



1
9
1

Fig. 4 Details of booster rod and suspension

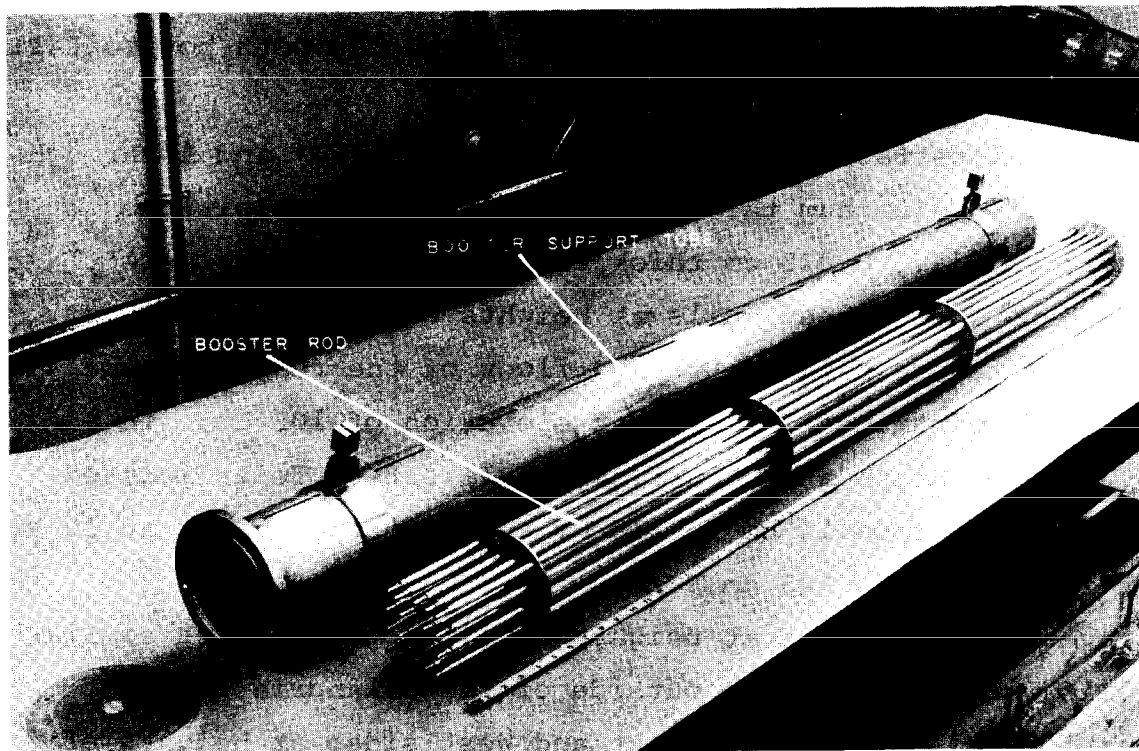


Fig. 5 BLW booster and support tube

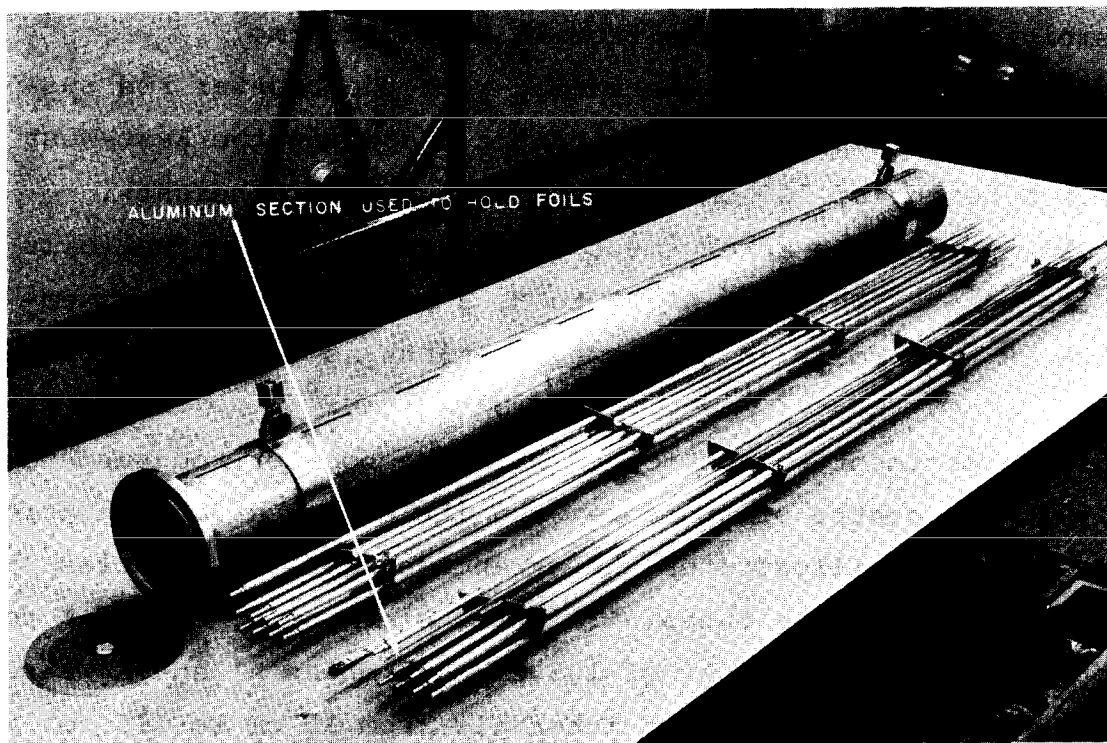


Fig. 6 BLW booster dismantled

was present, and when the booster rod was suspended both horizontally and vertically in the core.

Figure 7 illustrates the unperturbed lattice; A' and A through N are thin-walled aluminum thimbles at cell boundary positions holding 1.13 cm dia., 0.025 cm thick copper foils. Thimbles A', A to E and K to N contained foils at heights of 105 cm and 155 cm [all measurements are relative to the floor of the reactor vessel]; thimbles F to J contained foils at an elevation of 105 cm. In addition thimbles A', A and E carried a full set of foils located at 10 cm intervals from 15 cm to 215 cm and thimble J a set at 10 cm intervals from 65 cm to 145 cm.

To investigate effects at neighbouring fuel assemblies similar copper foils were taped to the outside of the calandria tubes of fuel assemblies F1 to F9 on the East and West sides at heights of 105 cm and 155 cm. In addition, foils were placed on the South side of assembly F1 at these two elevations, and along the North side of this assembly at 10 cm intervals from 15 cm to 215 cm.

The second experiment was performed with the booster rod suspended symmetrically about the core centre and along the East-West diameter at a height of 105 cm (close to the mid-core height). Figure 8 illustrates the arrangement of the thimbles and the foils on calandria tubes. Thimbles A', A to E, J and K to N, and assemblies F1 to F9 held foils in the same locations as in the unperturbed lattice.

A third experiment was performed with the booster rod suspended vertically at the centre of the core with its centre at an elevation of 105 cm. Figure 9 illustrates the arrangement of the thimbles and the foils on calandria tubes. Thimbles A', A to D, E' and K to N held copper foils at a height of 105 cm. Thimbles A' and E' also contained a set of foils at 10 cm intervals from 15 cm to 215 cm. In this experiment thimble E could not be used because of the

- 28 ROD BUNDLE
- 7 ROD BUNDLE
- ZEEP FUEL ASSEMBLY
- X FOIL THIMBLES
- ◌ FOILS ON CALANDRIA TUBE

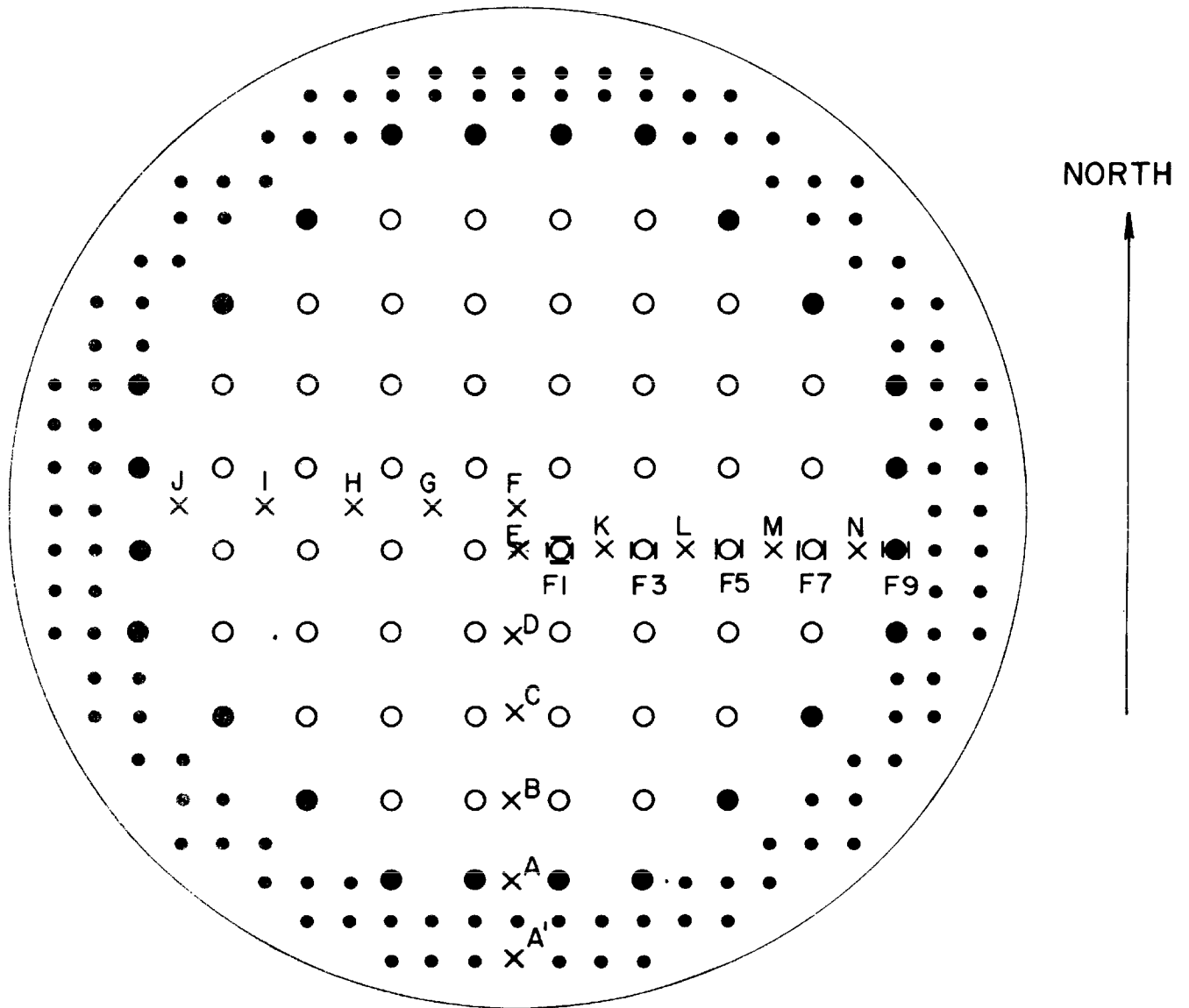


Fig. 7 BLW reference lattice arrangement in ZED-2

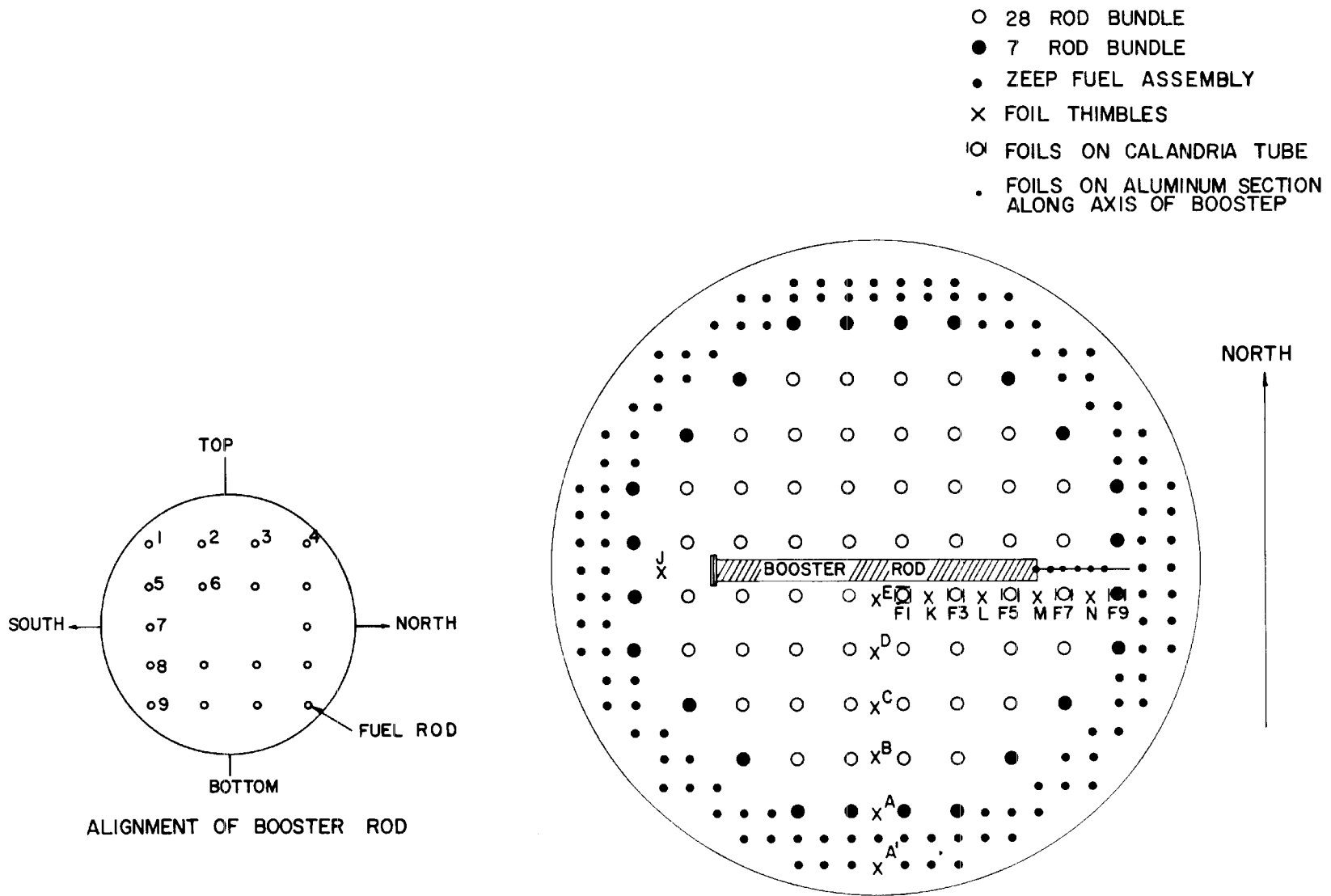


Fig. 8 BLW booster horizontal in ZED-2

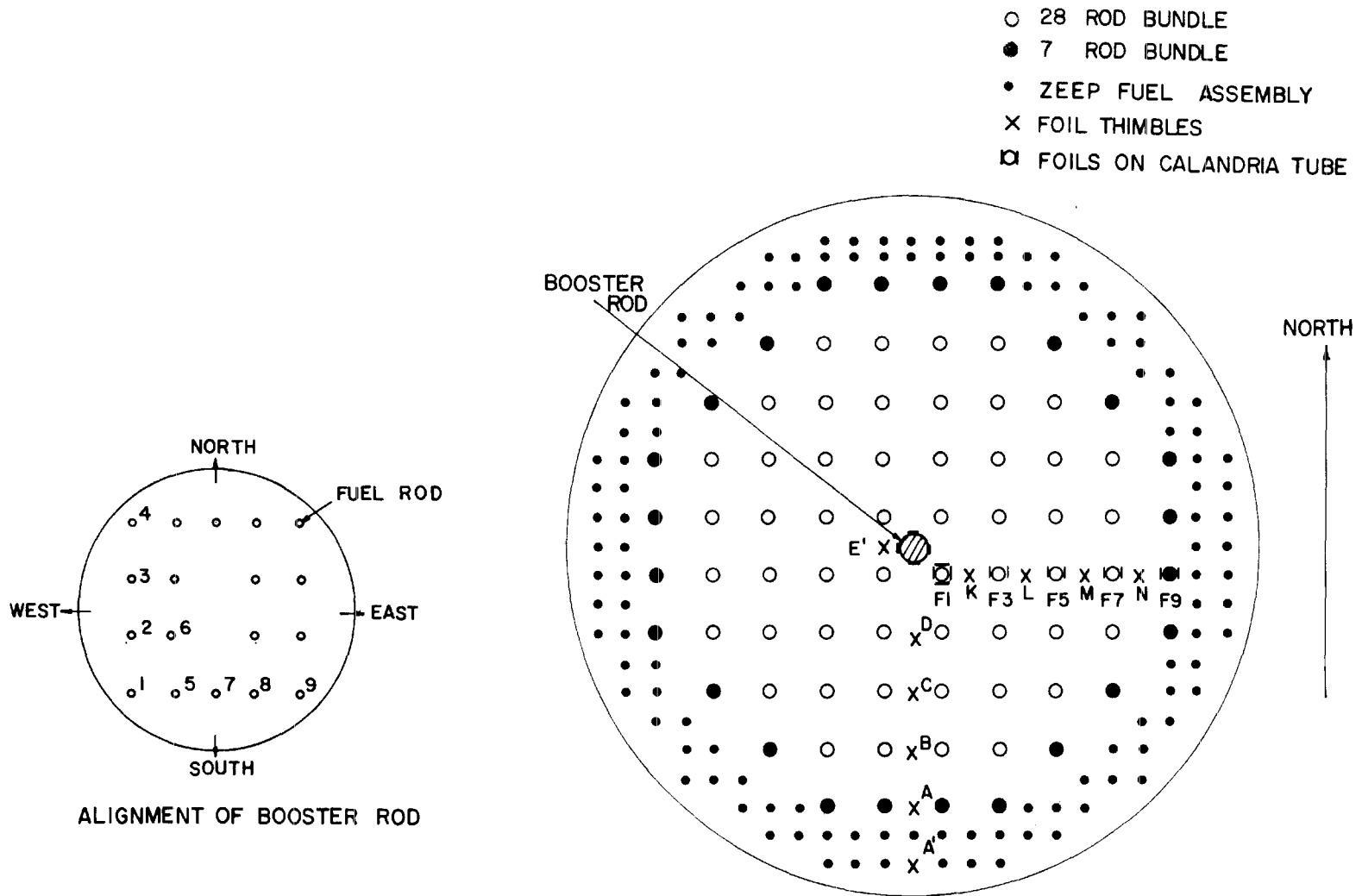


Fig. 9 BLW booster vertical in ZED-2

suspension system of the booster rod, it was replaced by thimble E¹ which is at the same cell location and same core radius as thimble E.

Foils were taped to the East and West sides of the calandria tube of assemblies F1 to F9 and the South side of F1, at an elevation of 105 cm. In addition the North side of the calandria tube of F1 held a set of copper foils at 10 cm intervals from 15 cm to 215 cm.

2. Detailed Neutron Density Measurements at Booster Rod

Figures 8 and 9 illustrate the location and orientation of the booster rod when suspended horizontally and vertically in the simulated BLW core.

When suspended horizontally in the lattice the booster held a long aluminum section at its centre along the longitudinal axis which extended ~ 19" beyond the East end of the booster (see Figure 6). This aluminum strip held copper foils at the locations indicated on Figure 8 at radii given in Table 8. Copper strips 5 mm wide and 0.010" thick were wrapped around the circumference of fuel rods #1 to #9 (see Figure 8) and four copper foils were taped to the support tube, in a North-South plane through the booster rod mid length (see Table 8). A gold wire 0.010" dia. and ~ 20 cm long was attached along the East end of rod #1.

When suspended vertically, fuel rods #1 to #9 (see Figure 9) held copper strips, and copper foils were taped to the North, South, East and West sides of the support tube, all at 105 cm elevation.

3. Neutron Spectrum Measurements

To compare the perturbed and unperturbed distributions accurately it was necessary to correct the measured foil relative activities for epithermal neutron activation to give relative total neutron densities.

In the BLW region of the unperturbed core $r\sqrt{T_n/T_0}$ values were known at various cell locations from previous measurements. Additional measurements were made at thimble A' and the calandria tube of F9 using pairs of indium and copper foils and comparing their activity ratio with the activity ratio of a similar pair of foils in thimble A where $r\sqrt{T_n/T_0}$ was determined by an indium cadmium-ratio measurement.

In the perturbed lattice, with the booster horizontal, spectrum measurements were made at thimbles A', D, E, and J, at the calandria tube of F1 (all at 105 cm elevation), at the centre of the booster, and on rod #1 at the East end of the booster (adjacent to the gold wire), using pairs of gold and copper foils and comparing their activity ratios to that of a similar pair of foils in thimble A where $r\sqrt{T_n/T_0}$ was obtained by an indium cadmium-ratio measurement.

With the booster vertical, similar measurements were made at thimble A', the calandria tube of F1, the centre of the booster (foils taped to a light aluminum support) and on rod #1 of the booster, all at 105 cm elevation.

4. Reactivity Measurements

In the reactivity measurements the lattice was similar to that of Figure 2 but it contained 120 ZEEP fuel assemblies; the last row of ZEEP assemblies on the South side of the lattice contained a fuel assembly in the central position (i.e. the position occupied by thimble A' in Figure 7).

Pile critical heights were determined for the following conditions:

- (a) Bare pile
- (b) Bare pile + cobalt wire
- (c) Booster rod suspension system, vertical in pile
- (d) Booster rod + suspension system, vertical in pile

- (e) Booster rod suspension system, horizontal in pile
- (f) Booster rod + suspension system, horizontal in pile

In (b) a 0.100" diameter cobalt wire extended axially through the moderator at the centre of the core; it served to calibrate the pile for relative reactivity changes.

In experiments (d) and (f) the booster was located in the core at the same positions as in the neutron density measurements described in Sect. III-1 above.

IV. RESULTS AND DISCUSSION

1. Lattice Neutron Density Perturbations

Relative foil activities $A(r,z)$ were converted to relative total neutron densities $n(r,z)$ using the expression $n(r,z) \propto A(r,z) / (G_{th}g + G_{r s_o} r\sqrt{T_n/T_o})$, where for the foils used $G_{th}g$ and $G_{r s_o}$ are known, (G_r, G_{th} are the resonance and thermal neutron self-shielding factors). For the perturbed lattice $r\sqrt{T_n/T_o}$ values are assumed to be the same as in the unperturbed lattice at distances > 50 cm from the booster rod. At other positions the measured values were used (see Table 1). At positions < 50 cm from the booster rod where measurements were not made, $r\sqrt{T_n/T_o}$ values were obtained by use of a plot of $n(r,z) \times r\sqrt{T_n/T_o}$ vs distance from booster. Interpolation between points at which measurements were made led to negligible error since the epithermal activation was $< 4\%$ of the thermal activation at all points.

The resulting relative total neutron densities in the unperturbed and perturbed lattices normalized to 1000 in thimble A' at an elevation of 105 cm are given in Tables 2 to 4.

TABLE 1: SUMMARY OF $r\sqrt{T_n/T_o}$ VALUES

Location	$r\sqrt{T_n/T_o}$	Method
<u>UNPERTURBED LATTICE</u>		
Thimble A	0.0272	a) Indium-Cadmium Ratio
Thimble A'	0.0259	Cu-In Activity Ratio relative to a)
Assembly F9-West	0.0369	"
Thimbles B to I	0.0210	Indium-Cadmium Ratio Measurements in BLW(AS) Lattice
Thimble J	0.0285	"
<u>BOOSTER ROD HORIZONTAL</u>		
Thimble A	0.0270	b) Indium-Cadmium Ratio
Thimble A'	0.0233	Au-Cu Activity Ratio Relative to b)
Thimble D	0.0220	"
Thimble E	0.0326	"
Thimble J	0.0176	"
Assembly F1-North	0.0581	"
Centre of Booster	0.0848	"
Rod #1 of Booster	0.0500	"
<u>BOOSTER ROD VERTICAL</u>		
Thimble A	0.0278	c) Indium-Cadmium Ratio
Thimble A'	0.0228	Au-Cu Activity Ratio Relative to c)
Assembly F1-North	0.0878	"
Centre of Booster	0.0801	"
Rod #1 of Booster	0.0389	"

TABLE 2: NORMALIZED TOTAL NEUTRON DENSITIES - B L W (AT) LATTICE UNPERTURBED

Location	ELEVATION ABOVE FLOOR OF CALANDRIA (cm)																				
	15	25	35	45	55	65	75	85	95	105	115	125	135	145	155	165	175	185	195	205	215
A'	425	502	591	679	760	831	892	940	977	1000	1010	1007	991	961	919	865	800	724	638	545	442
A	508	611	724	840	945	1037	1115	1178	1225	1256	1269	1265	1244	1206	1152	1082	997	899	788	669	540
B										1321					1218						
C										1272					1177						
D										1249					1156						
E	489	580	690	799	906	1001	1081	1147	1196	1229	1245	1243	1224	1187	1136	1068	985	888	779	657	531
F										1343											
G										1353											
H										1383											
I										1438											
J						1242	1336	1419	1475	1514	1527	1527	1494	1451							
K										1243					1148						
L										1291					1170						
M										1298					1198						
N										1383					1278						
F1 N	415	460	546	632	719	806	842	874	920	940	955	950	940	920	887	858	768	686	604	517	424
S										955					875						
E										969					863						
W										937					905						
F3 E										988					863						
W										944					907						
F5 E										991					927						
W										988					898						
F7 E										1052					973						
W										1011					928						
F9 E										705					602						
W										841					699						

TABLE 3: NORMALIZED TOTAL NEUTRON DENSITIES - BLW BOOSTER HORIZONTAL

Location	ELEVATION ABOVE FLOOR OF CALANDRIA (cm)																				
	15	25	35	45	55	65	75	85	95	105	115	125	135	145	155	165	175	185	195	205	215
A'	459	539	635	724	805	874	928	968	992	1000	992	969	930	876	808	727	634	532	420	293	144
A	565	678	799	920	1040	1126	1196	1248	1283	1294	1283	1255	1193	1132	1035	930	800	658	513	350	163
B										1426					1144						
C										1499					1180						
D										1693					1262						
E	662	794	965	1145	1323	1515	1679	1825	1877	1851	1888	1864	1719	1543	1365	1193	1000	809	614	414	197
J						1457	1559	1636	1696	1708	1700	1640	1567	1471							
K										1817					1346						
L										1729					1297						
M										1605					1227						
N										1565					1239						
F1 N	551	623	749	894	1044	1204	1304	1401	1372	1119	1345	1410	1321	1188	1059	947	781	623	475	326	162
S										1459					1010						
E										1402					1015						
W										1381					1064						
F3 E										1338					969						
W										1366					1057						
F5 E										1243					968						
W										1280					980						
F7 E										1210					950						
W										1220					941						
F9 E										749					528						
W										914					630						

TABLE 4: NORMALIZED TOTAL NEUTRON DENSITIES - BLW BOOSTER VERTICAL

Location	ELEVATION ABOVE FLOOR OF CALANDRIA (cm)																				
	15	25	35	45	55	65	75	85	95	105	115	125	135	145	155	165	175	185	195	205	215
A'	453	535	630	715	796	865	921	962	989	1000	996	977	942	893	831	755	668	571	464	349	214
A										1276											
B										1396											
C										1471											
D										1669											
E'	724	863	998	1163	1333	1483	1588	1670	1742	1774	1772	1722	1648	1555	1425	1271	1099	934	750	539	316
K										1768											
L										1555											
M										1412											
N										1424											
F1 N	618	694	814	947	1092	1231	1272	1326	1369	1381	1416	1352	1298	1232	1137	1039	880	738	592	430	263
S										1405											
E										1416											
W										1377											
F3 E										1238											
W										1298											
F5 E										1097											
W										1158											
F7 E										1088											
W										1079											
F9 E										698											
W										837											

Figure 10 illustrates radial neutron density distributions in various directions in the unperturbed core. Due to the low reactivity of the BLW region and the surrounding 'driver' region, the distribution follows an I_0 function at radii $< \sim 100$ cm. Figure 11 illustrates corresponding distributions in the two perturbed lattices.

Axial neutron density distributions in the unperturbed and the perturbed lattices are given in Figures 12 and 13. These figures illustrate the effect of the booster rod on the lattice. As expected, the presence of the booster increases the total neutron density over the lattice whilst the strong thermal neutron absorption of the ^{235}U causes a local depression of the neutron density near the booster.

To discuss these perturbation effects quantitatively we define a flux perturbation factor $F(r,z)$ where

$$F(r,z) = \frac{\left[\frac{n(r,z)}{n(R,z)} \right]_{\text{perturbed}}}{\left[\frac{n(r,z)}{n(R,z)} \right]_{\text{unperturbed}}}$$

$n(r,z)$ and $n(R,z)$ are the relative total neutron densities at points having co-ordinates r, z and at the same height z at radius R of thimble A' respectively. Thimble A' was chosen as the reference position since it is a large distance away from the source of perturbation (\sim ten migration lengths), and should be essentially unaffected by it. The validity of this assumption is indicated by Figures 14 and 19 where $F(r,z)$ decreases smoothly to 1.0 at thimble A'. Furthermore, the results of least squares cosine fits to the activity distributions obtained at thimble A' in the perturbed and unperturbed lattices gave values of δ'_z , a measure of the total axial extrapolation length, which agree well within the limits of error (see Table 7).

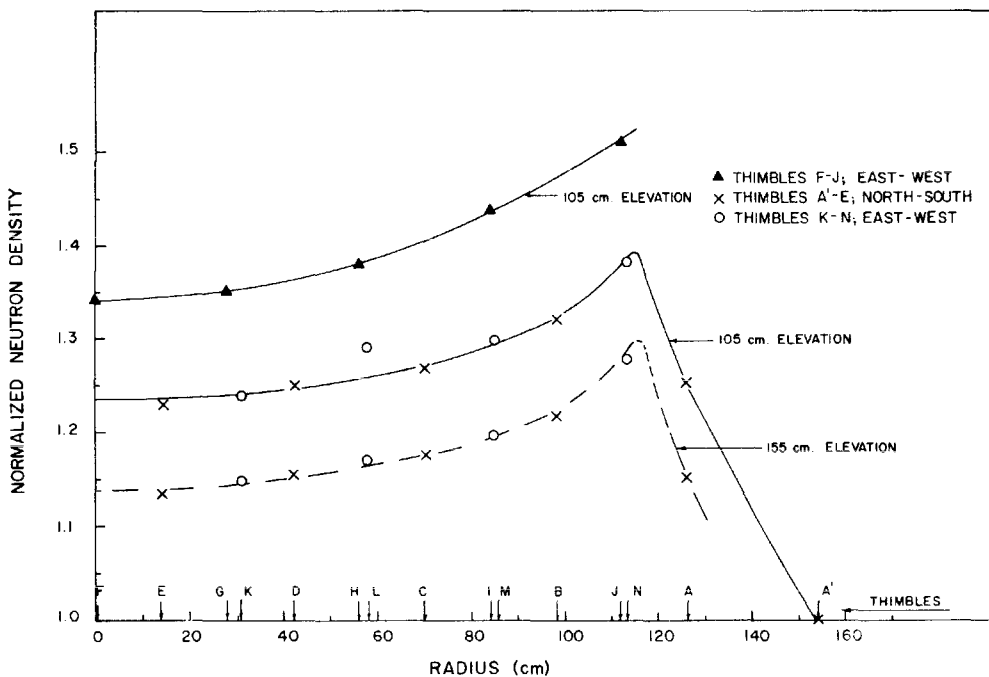


Fig. 10 Radial normalized neutron density distributions in unperturbed lattice: foils in thimbles

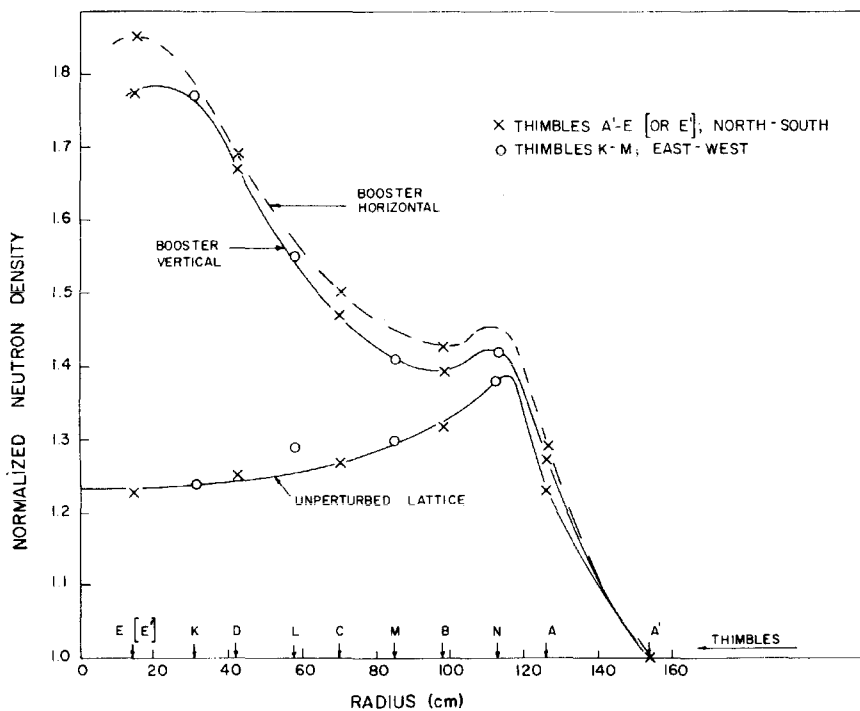


Fig. 11 Radial normalized neutron density distributions in unperturbed and perturbed lattices

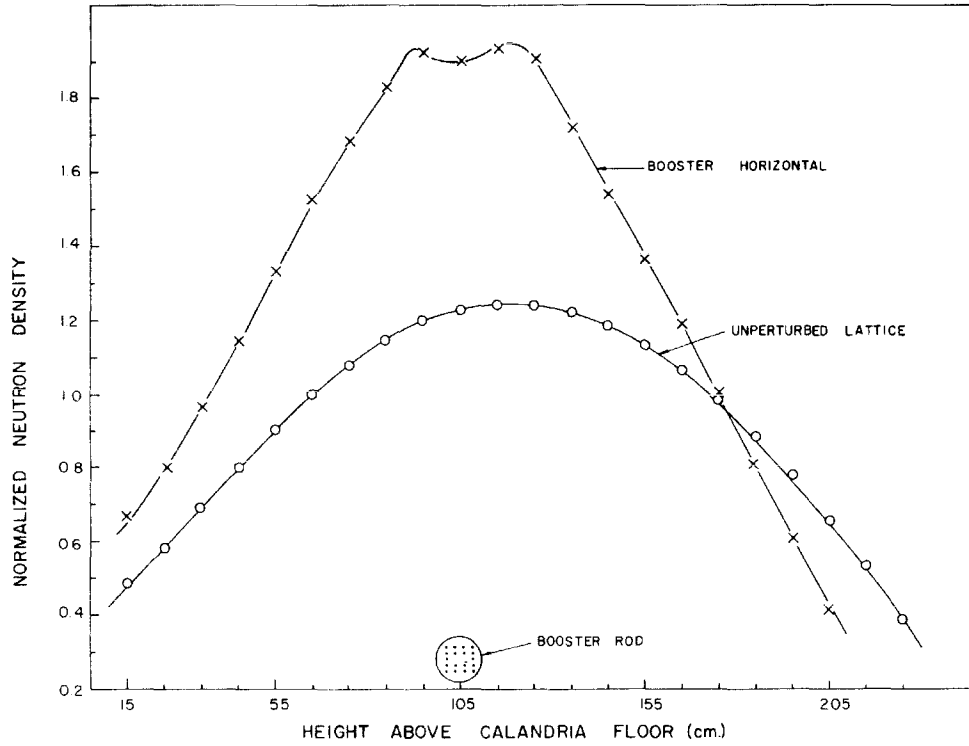


Fig. 12 Axial relative total neutron density distribution; thimble E

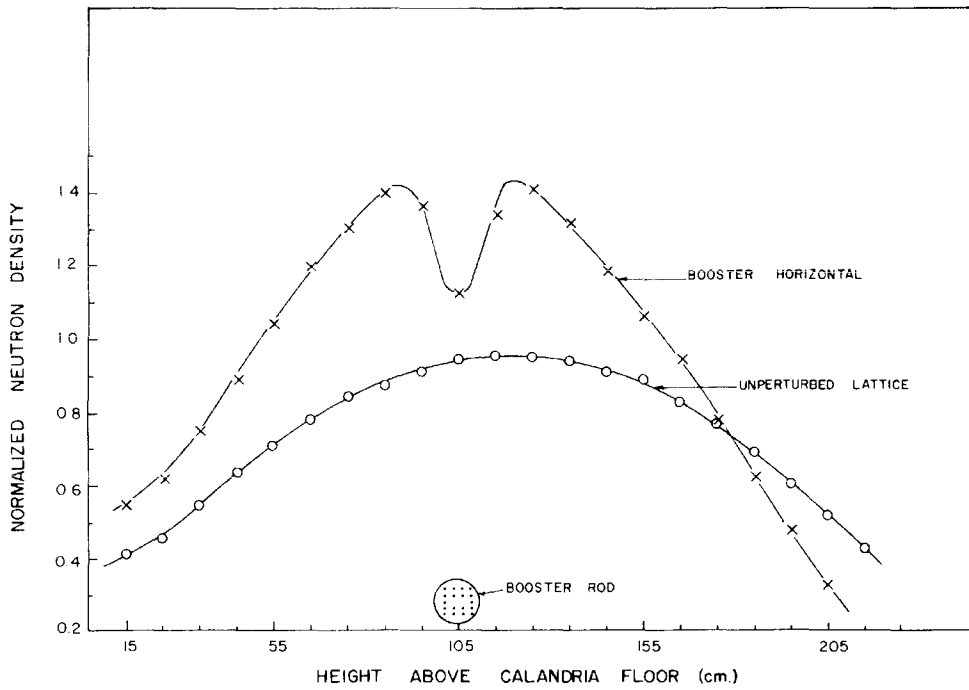


Fig. 13 Axial relative total neutron density distributions; foils on north side of calandria tube of F1

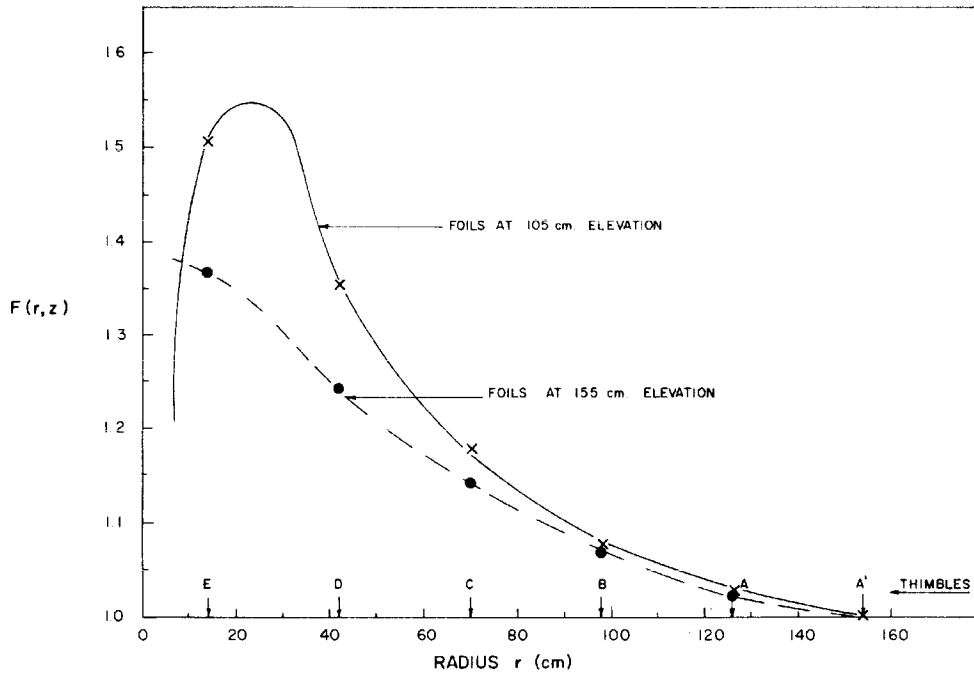


Fig. 14 Plot of $F(r,z)$ against radius; foils in thimbles, north-south direction; booster rod horizontal

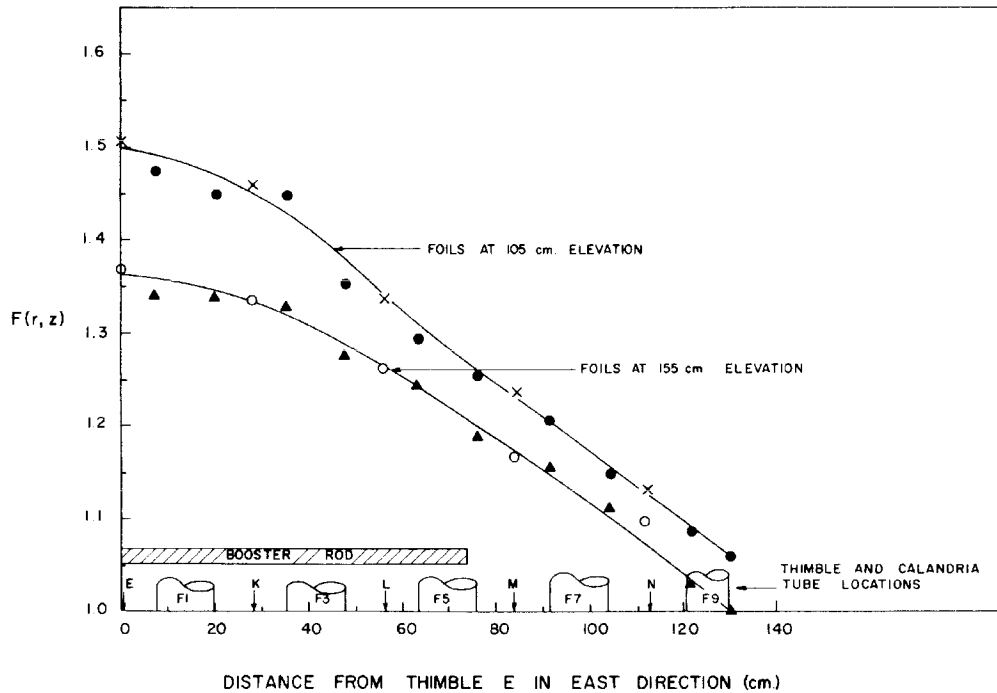


Fig. 15 Plot of $F(r,z)$ for foils in thimbles and on calandria tube in east-west direction: booster rod horizontal

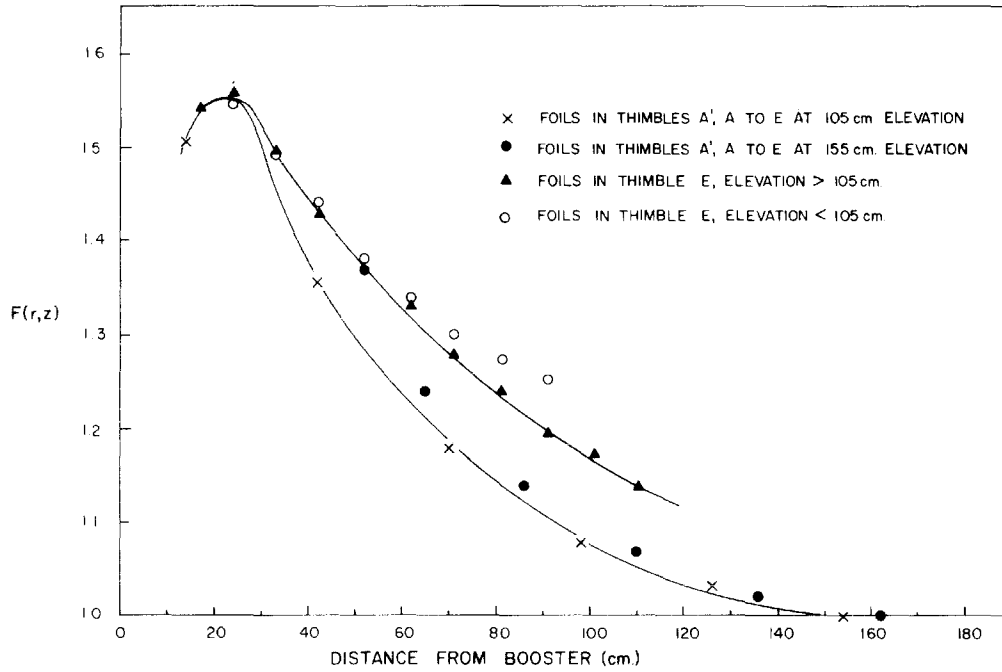


Fig. 16 Plot of $F(r,z)$ against distance from booster for foils in a north-south diametral plane; booster rod horizontal

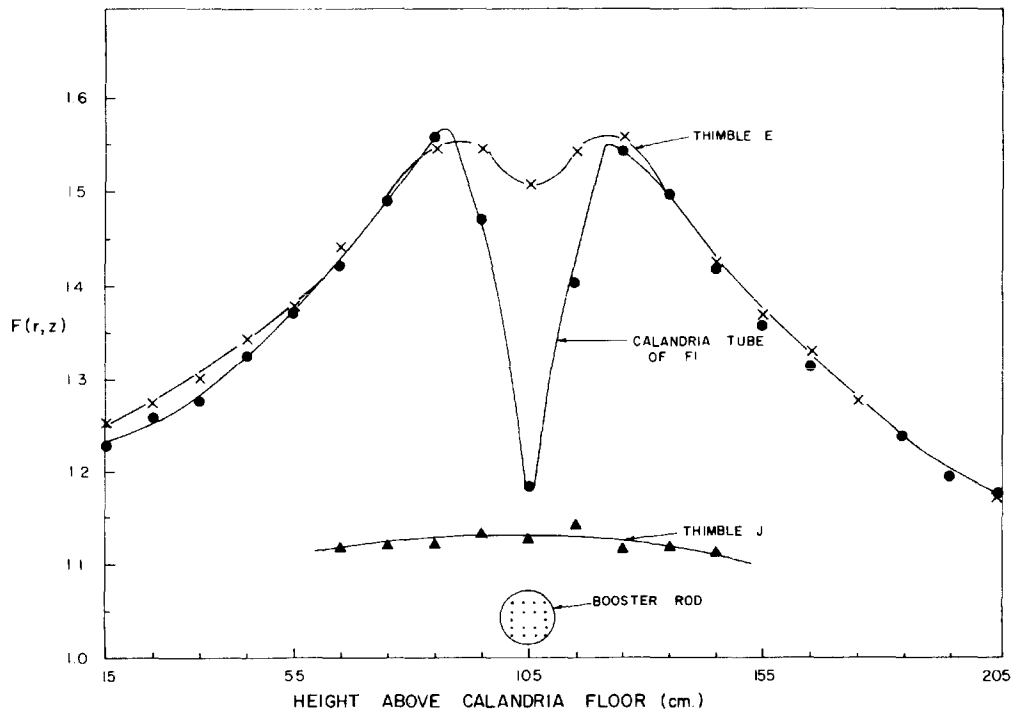


Fig. 17 Axial flux perturbation factors; booster rod horizontal

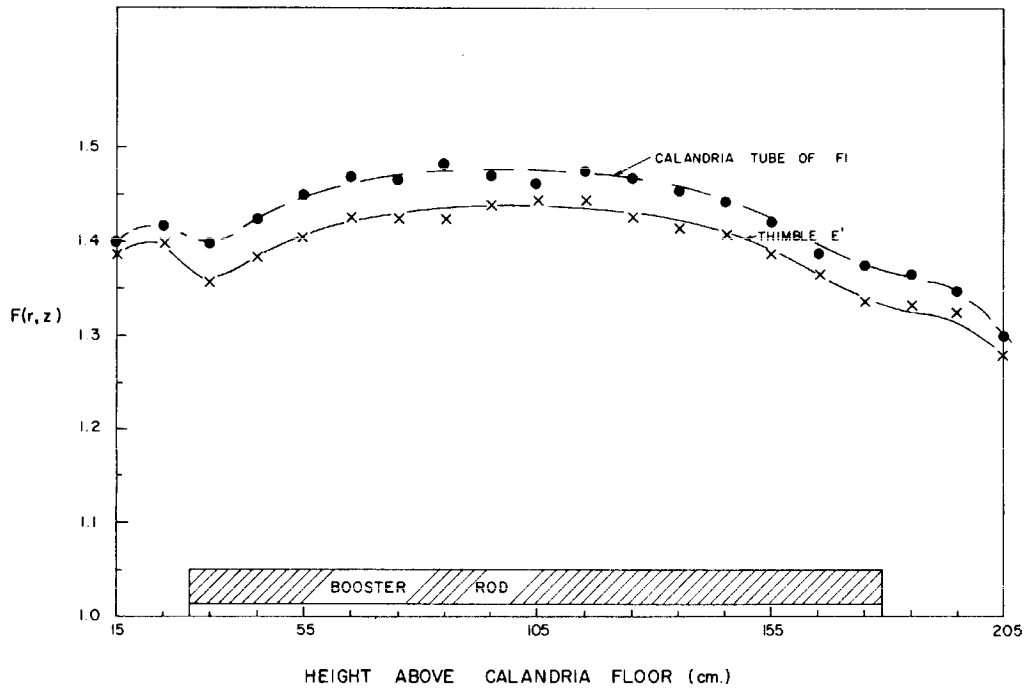


Fig. 18 Axial flux perturbation factors;
booster rod vertical

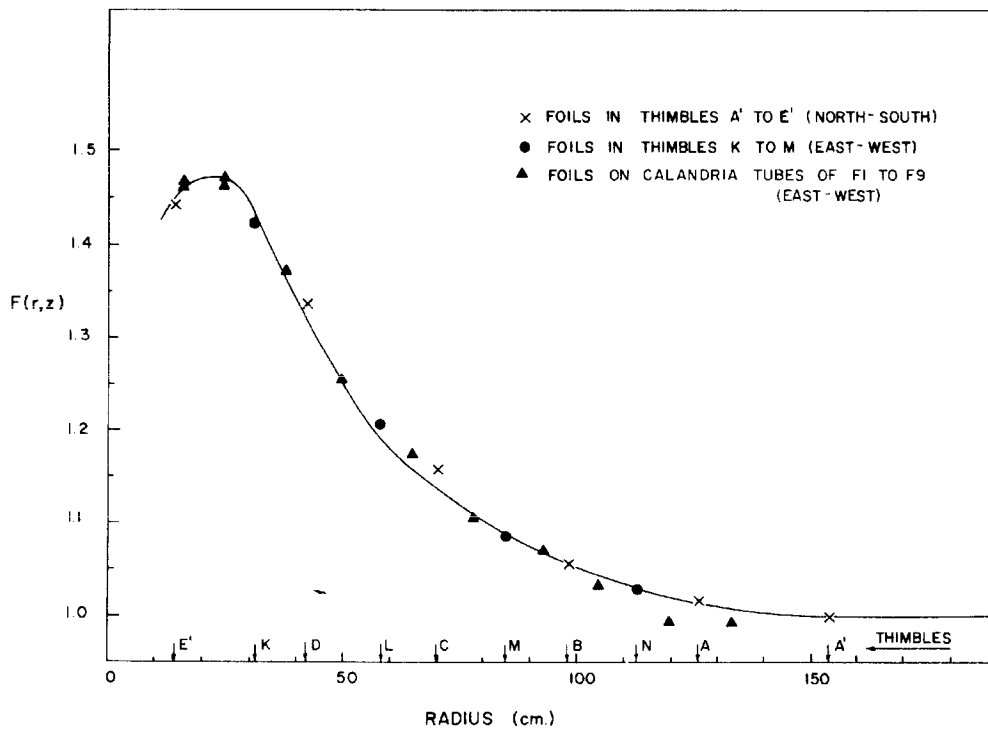


Fig. 19 $F(r,z)$ against radius at 105 cm. elevation;
booster rod vertical

Tables 5, 6 and 8 list the values of $F(r,z)$. Figures 14 to 17 illustrate the results for various directions in the core perturbed by the horizontal booster. Figures 14, 16 and 17 illustrate a large peaking of the total neutron density with a maximum $F(r,z) \sim 1.55$ at a distance ~ 20 cm from the booster. Near the booster the strong thermal neutron absorption severely depresses the neutron density (see Figure 17). Figure 16 plots $F(r,z)$ for all points on a North-South diametral plane through the core, against distance from the booster. This illustrates that the perturbation of the lattice is not the same in all directions about the booster.

When the booster is suspended vertically it extends from a height of ~ 31 cm to ~ 179 cm, i.e. it is almost a full length perturbation axially. Figure 18 illustrates $F(r,z)$ at thimble E' and the North side of assembly F1. Radial effects are illustrated in Figure 19 which uses all available data from foils in thimbles and on calandria tubes in various directions through the core. The curve shows a large flux peaking, a maximum $F(r,z) \sim 1.47$ occurring at a distance ~ 20 cm from the booster.

2. Neutron Density Measurements at Booster Rod

(a) General

Table 8 lists normalized relative total neutron densities for the foils on the booster rod and suspension tube when the booster is both horizontal and vertical. Also listed in Table 8 are $F(r,z)$ values for foils along the axis of the booster; these values are illustrated in Figure 20. The strong thermal absorption in the ^{235}U depresses the neutron density within the booster, the perturbation factor along the axis of the booster varying between ~ 0.68 at the centre to ~ 0.63 , 42 cm along the booster (see Table 8, Figure 20). Beyond the end of the booster the $F(r,z)$ rises rapidly to a maximum of ~ 1.2 , at ~ 20 cm beyond the end of the fuel.

TABLE 5: FLUX PERTURBATION FACTORS $F(r, z)$ - BLW BOOSTER HORIZONTAL

Location	ELEVATION ABOVE FLOOR OF CALANDRIA (cm)																			
	15	25	35	45	55	65	75	85	95	105	115	125	135	145	155	165	175	185	195	205
A'	1.000	1.000	1.000	1.000	1.000	1.000	1.000	1.000	1.000	1.000	1.000	1.000	1.000	1.000	1.000	1.000	1.000	1.000	1.000	1.000
A	1.031	1.033	1.027	1.027	1.039	1.034	1.030	1.030	1.030	1.030	1.029	1.032	1.021	1.030	1.022	1.024	1.012	0.998	0.987	0.975
B										1.079					1.069					
C										1.179					1.141					
D										1.356					1.243					
E	1.253	1.275	1.301	1.344	1.378	1.441	1.493	1.547	1.545	1.506	1.544	1.559	1.496	1.426	1.368	1.330	1.279	1.239	1.195	1.173
J						1.116	1.121	1.121	1.132	1.128	1.142	1.116	1.117	1.113						
K										1.462					1.334					
L										1.339					1.263					
M										1.236					1.166					
N										1.131					1.104					
F1 N	1.228	1.260	1.276	1.326	1.371	1.421	1.489	1.558	1.469	1.185	1.404	1.544	1.497	1.418	1.358	1.314	1.281	1.236	1.193	1.177
S										1.527					1.314					
E										1.447					1.338					
W										1.474					1.339					
F3 E										1.354					1.278					
W										1.447					1.327					
F5 E										1.254					1.188					
W										1.295					1.243					
F7 E										1.150					1.112					
W										1.207					1.155					
F9 E										1.062					0.998					
W										1.087					1.026					

TABLE 6: FLUX PERTURBATION FACTORS $F(r, z)$ - BLW BOOSTER VERTICAL

Location	ELEVATION ABOVE FLOOR OF CALANDRIA (cm)																				
	15	25	35	45	55	65	75	85	95	105	115	125	135	145	155	165	175	185	195	205	215
A'	1.000	1.000	1.000	1.000	1.000	1.000	1.000	1.000	1.000	1.000	1.000	1.000	1.000	1.000	1.000	1.000	1.000	1.000	1.000	1.000	1.000
A										1.016											
B										1.057											
C										1.156											
D										1.336											
E a)	1.389	1.397	1.356	1.383	1.405	1.425	1.424	1.424	1.438	1.443	1.444	1.428	1.414	1.408	1.388	1.364	1.335	1.332	1.323	1.282	1.230
K										1.422											
L										1.204											
M										1.088											
N										1.030											
F1E N	1.398	1.415	1.397	1.423	1.450	1.468	1.464	1.482	1.469	1.462	1.473	1.467	1.452	1.441	1.418	1.387	1.371	1.365	1.346	1.300	1.282
S										1.471											
E										1.461											
W										1.469											
F3 E										1.253											
W										1.374											
F5 E										1.106											
W										1.173											
F7 E										1.034											
W										1.067											
F9 E										0.991											
W										0.996											

a) Based on neutron densities in thimble E of unperturbed lattice and thimble E' of perturbed lattice

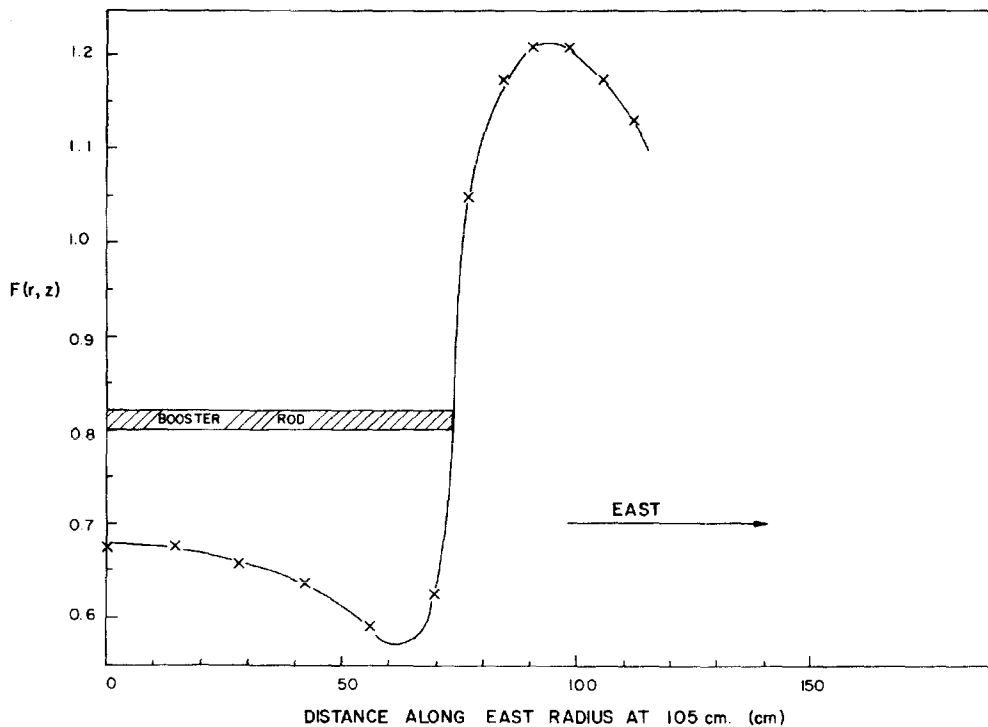


Fig. 20 Plot of $F(r, z)$ for foils along centre line of horizontal booster rod

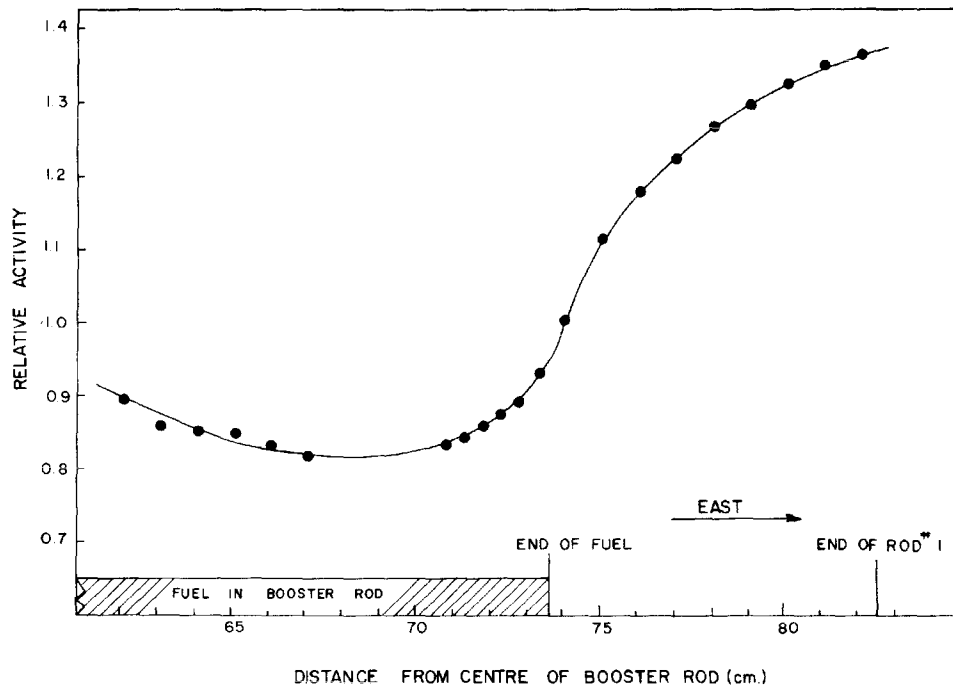


Fig. 21 Relative activity distribution, rod #1; booster rod horizontal

The detailed flux peaking at the end of a fuel rod is illustrated by the relative activities obtained from the gold wire on fuel rod #1, see Figure 21.

(b) Average Neutron Density in Booster Rod

From the neutron density measurements made at the sheaths of the fuel rods of the booster and at thimble F in the unperturbed lattice, and detailed neutron density measurements made in an unperturbed cell of this lattice (see Appendix A), we can determine

$$\frac{\bar{n}_s}{\bar{n}_{UO_2}} = \frac{\bar{n}_s}{n_F} \cdot \frac{n_F}{\bar{n}_{UO_2}}$$

where \bar{n}_s and \bar{n}_{UO_2} are the average neutron densities at the sheaths of the 18 fuel rods of the booster in a plane perpendicular to the booster at its mid length (see Table 8), and the average neutron density in the UO_2 fuel of the simulated unperturbed BLW lattice respectively (see Appendix A). n_F is the relative neutron density at thimble F (a cell corner location), elevation 105 cm, in the unperturbed lattice.

From Tables 2 and 8

$$\frac{\bar{n}_s}{n_F} = 0.695$$

From Appendix A $\frac{n_{\text{cell corner}}}{\bar{n}_{UO_2}} = \frac{n_F}{\bar{n}_{UO_2}} = 2.65$

Therefore $\frac{\bar{n}_s}{\bar{n}_{UO_2}} = 1.84$

Note: When the booster is perpendicular to the fuel assemblies a cell average value of the above ratio must take into account

the cell neutron density fine structure. Using the results of Figure A1 of Appendix A we obtain for the horizontal booster a cell average value of

$$\frac{\bar{n}_s}{\bar{n}_{UO_2}} \Bigg|_{\text{Cell Av.}} = 1.75 \quad (1)$$

Kushneriuk's 'blackness' theory has been used to estimate the ratio of the neutron density at the surface to the average neutron density in a fuel rod of the booster, \bar{n}_{235} , (see Appendix B), and ignoring flux depression through the aluminum sheath,

$$\frac{\bar{n}_s}{\bar{n}_{235}} = 1.18 \quad (2)$$

Assuming the above ratio is applicable to each fuel rod of the booster, then combining expressions (1) and (2) we can obtain an estimate of the ratio of the average neutron density in the fuel of the booster rod to the average neutron density in the fuel of the unperturbed lattice, for the booster perpendicular to the assemblies of the lattice;

$$\frac{\bar{n}_{235}}{\bar{n}_{UO_2}} \Bigg|_{\text{Cell Av.}} \approx 1.5$$

3. Reactivity Measurements

Because of the multi-zone nature of the reactor core it is not readily possible to calibrate the pile in terms of absolute reactivity changes using the cobalt wire technique.

The results of the reactivity measurements expressed in terms of changes in axial buckling ΔB_z^2 are listed on Table 9 where

$$\Delta B_z^2 = \pi^2 \left[\frac{1}{(H_c + \Delta H_c)^2} - \frac{1}{H_c^2} \right]$$

H_c is the extrapolated unperturbed pile critical height $\left[= H_{D_2O} \text{ (the heavy water critical height)} + \delta'_z \right]$, where $\delta'_z = 22.06$ cm as determined from previous experiments].

ΔH_c is the change in pile critical height due to the perturbation.

Table 9 lists values of H_c , ΔH_c and ΔB_z^2 for all experiments. All results are expressed at a temperature of 22.25°C and a heavy water purity of 99.963 a/o D_2O .

V. REACTIVITY MEASUREMENTS; A COMPARISON WITH CALCULATION

These calculations were performed as a check on the ability to calculate such reactivity effects using perturbation theory. Because of the multi-zone nature of the lattice used in these experiments it is not readily possible to calculate the absolute reactivity changes caused by the cobalt wire or the booster rod. However, comparison can be made between predicted relative reactivity changes, δk , and the measured changes in axial buckling, ΔB_z^2 , since

$$\delta k_\infty = F(h) (L^2 + L_s^2 + 2L^2 L_s^2 B^2) \Delta B_z^2$$

i.e. $\delta k_\infty = A \Delta B_z^2$ (3)

$F(h)$ is a factor which expresses the change in radial buckling with critical height for this lattice.

L^2 , L_s^2 and B^2 have their usual meanings.

It is assumed that A remains constant under the various perturbations.

TABLE 9: LATTICE REACTIVITY DATA

Experiment	H_c cm	ΔH_c cm	ΔB_z^2 m^{-2}
Cobalt Wire	265.257	+0.776	-8.17×10^{-3}
Suspension system Vertical	265.237	+0.685	-7.21×10^{-3}
Booster Vertical	265.200	-21.380	$+25.69 \times 10^{-2}$
Suspension system Horizontal	265.292	+1.260	-1.32×10^{-2}
Booster Horizontal	265.267	-25.716	$+31.73 \times 10^{-2}$

The reactivity effect of inserting a highly enriched booster rod at an interstitial position in the lattice is essentially composed of two terms, a reduction in the neutron density at the booster due to the thermal neutron absorption in the ^{235}U and in the structural material (aluminum) of the booster, and an increase in the neutron density about the booster due to the neutron production by the ^{235}U . Resonance absorption in the ^{238}U of the booster rod is negligible because of its low relative concentration.

Perturbation theory enables us to express the net reactivity effect as

$$\frac{\delta k}{k} = \frac{\int_{\text{Booster}} \left[\nu \Sigma_F W_f \phi'_t - \left[\frac{\Lambda}{\Sigma_a} W_t \phi'_t \right]_{235} - \left[\frac{\Lambda}{\Sigma_a} W_t \phi'_t \right]_{\text{Al}} \right] dv}{\int_{\text{Lattice}} \left(\nu \Sigma_F W_f \phi_t \right)_U dv} \quad (4)$$

where the subscripts F, f, t, 235, Al, U refer to fission, fast, thermal, ^{235}U , aluminum and the natural uranium fuel of the lattice, respectively. ϕ and W are the neutron flux and importance respectively and the prime refers to a value in the perturbed lattice. V is volume.

$\phi \equiv 1$ at the centre of the unperturbed lattice; $(r, z) = (0, 105)$.

We assume that

$$W_f = W_t \cdot \frac{p}{1 + L_s^2 B^2}$$

and that the importance, W_t , is proportional to the flux ϕ_t ; also that W_t shows no fine structure in a cell.

Note that equation (4) only includes terms weighted by flux, terms weighted by flux gradient are ignored.

Rearrangement of equation (4) gives

$$\delta k = c \left[\left\{ \frac{\nu \Sigma_{fP}}{1 + L_s^2 B^2} - \left(\frac{\Lambda}{\Sigma_a} \right)_{235} - \left(\frac{\Lambda}{\Sigma_a} \right)_{Al} \right\} \cdot a \int_{\text{Booster}} \phi_t \phi_t' d\ell \right] \quad (5)$$

where " ℓ " is the distance along the longitudinal axis of the booster from the booster mid length and "a" is the geometric cross sectional area of the fuel in the booster. C is a constant of the lattice.

From Figures 18 and 20 we know that $F(r,z)$ is not constant along the booster, the integral of equation 5 can therefore be written as

$$\int_{\text{Booster}} \phi_t \phi_t' d\ell = b \int_{\text{Booster}} \frac{F(\ell)}{F(0)} \phi_t^2(\ell) d\ell = 0 \quad (6)$$

where b is the ratio of the average total neutron density in the fuel of the booster rod in a plane through the booster rod at $\ell = 0$ and perpendicular to its long axis, to the total neutron density at the location $(r,z) = (0, 105)$ in the unperturbed lattice.

$$\text{i.e. } b = \frac{\bar{n}_{235}}{n_F} (\ell = 0)$$

Note that for the horizontal booster "b" must include cell fine structure effects.

Values of "b" were obtained using the measured relative total neutron densities at the surface of the 18 fuel rods of the booster, see Tables 2 and 8, a ratio of average neutron density in the fuel to neutron density at the surface of a fuel rod, calculated using Kushneriuk's 'blackness' method⁽⁷⁾ (see Appendix B), and the detailed neutron density distributions of Appendix A.

$F(l)/F(0)$ is the ratio of the flux perturbation factors at a location " l " along the booster and at the centre of the booster rod, evaluated using the experimental results of Figures 18, 20 and 21.

Inserting into equation (5) suitable values of ν , Σ_f , Σ_a , values of p and L^2 calculated for a 28 rod lattice using LATREP⁽⁸⁾, and values of B^2 and 'Q' from experiment, we obtain

$$[\delta k]_{\text{vertical}} = +492 \text{ C milli-k}$$

Applying equation (4) to a cobalt wire (a pure absorber) passing axially through the centre of the lattice we obtain

$$\delta k_{\text{Co}} = C \cdot (\Sigma_a^{\Lambda} V)_{\text{Co}} \phi_t^2$$

For the wire used in these experiments

$$(\Sigma_a^{\Lambda} V)_{\text{Co}} = 27.90 \text{ cm}^2$$

Hence

$$\delta k_{\text{Co}} = 14 \text{ C milli-k}$$

Comparing this reactivity effect with that calculated for the booster rod vertical in the lattice we obtain

$$\frac{[\delta k]_{\text{vertical}}}{\delta k_{\text{Co}}} = \frac{+492}{-14} = \underline{\underline{-35}}$$

This compares favourably with the equivalent experimental ratio (see equation 1, Table 9) of

$$\frac{[\Delta B_z^2]_{\text{vertical}}}{[\Delta B_z^2]_{\text{Co}}} = \frac{+26.6}{-0.817} = \underline{\underline{-32.6}}$$

VI. STATISTICAL WEIGHT THEORY APPLIED TO THE ROTATION OF THE BOOSTER ROD

Comparison can also be made between the relative reactivity effects of the booster horizontal and vertical in the lattice as

predicted using statistical weight theory, and the corresponding measured values of changes in axial buckling.

Using equation (6) and values of 'Q' based on the experimental results obtained with the booster horizontal and vertical we obtain

$$\frac{[\delta k]_{\text{horizontal}}}{[\delta k]_{\text{vertical}}} = \frac{Q_{\text{horizontal}}}{Q_{\text{vertical}}} = \underline{\underline{1.30}}$$

This ratio can be compared (see equation 3 and Table 9) with

$$\frac{[\Delta B_z^2]_{\text{horizontal}}}{[\Delta B_z^2]_{\text{vertical}}} = \frac{33.1}{26.6} = \underline{\underline{1.24}}$$

Agreement is good between the calculated and experimental ratios indicating the applicability of the theory to describe the rotation.

VII. CONCLUSIONS

Experiments have been performed using a simulated CANDU-BLW core in ZED-2 to investigate the reactivity effects and the perturbing effect on the surrounding lattice when a mock-up BLW Booster rod is inserted into the lattice both parallel and perpendicular to the fuel assemblies.

The booster rod acted as a large source of neutrons and raised the overall neutron density in the lattice, a maximum increase in the neutron density $\sim +55\%$ occurring ~ 20 cm away from the booster when it was horizontal in the lattice. When the booster was vertical in the lattice the perturbation was $\sim +47\%$ and again occurred ~ 20 cm from the booster.

At the booster the strong thermal neutron absorption in the ^{235}U depresses the neutron density, a depression in the neutron density along the axis of the booster relative to the unperturbed

density of $\sim 35\%$ being observed.

Detailed neutron density measurements at the cladding of the 18 fuel rods of the booster combined with 'blackness' calculations and detailed neutron density distributions in an unperturbed cell of the 28-rod lattice, gave an estimate of the neutron densities in the ^{235}U fuel rods relative to the UO_2 fuel of the simulated BLW lattice.

Results of reactivity measurements made with the booster parallel and perpendicular to the fuel assemblies of the lattice are expressed in terms of changes in axial buckling relative to the effect of a standard cobalt absorber in the lattice.

A perturbation theory calculation of the relative reactivity effects of the booster and the standard absorber was in fair agreement with the equivalent experimental value.

The application of statistical weight theory to the relative reactivity effects of the booster parallel and perpendicular to the fuel assemblies of the lattice gave good agreement with experiment. This indicates the applicability of the theory to describe this rotation.

Although the results obtained for neutron density perturbations, relative reactivities and relative neutron densities in the fuel of the booster are not directly applicable to the BLW reactor, due to differences in the lattice, operating conditions, and design of the booster, they do serve as a useful normalization of the theories used to describe these problems.

ACKNOWLEDGEMENTS

The author wishes to thank the many people involved in performing the experiments and producing this report, in particular to P.D.J. Ferrigan, E. Pleau and D.J. Roberts who arranged the thimbles, foils and booster rod in the reactor, J.T.R. Young and A. Teitsma who counted the foils and wires, Miss D. Graham who helped analyze the data, the typists of the stenographic services who typed the text and tables, Mrs. S. Argue who typed the final draft, and Dr. R.E. Green and Dr. C.H. Millar who gave advice on performing the experiments and criticised the manuscript.

REFERENCES

1. R.E. KAY and C.J. TANNER; CANDU-BLW Experiments in ZED-2 Part 1: Refuelling Experiment, AECL-2667 (1967).
2. ZED-2, AECL-2132 (1964).
3. G.A. PON; CANDU-BLW-250 Progress Report, AECL-2554 (1966).
4. K.J. SERDULA; Lattice Measurements with 28-Element Natural UO_2 Fuel Assemblies, Part 1: Bucklings for a Range of Spacings with Three Coolants, AECL-2606 (1966).
5. D.W. HONE et al.; Natural Uranium Heavy Water Lattices, Experiment and Theory, AECL-622 (1958).
6. R.E. GREEN et al.; Lattice Studies at Chalk River and their Interpretation, AECL-2025 (1964).
7. S.A. KUSHNERIUK; Neutron Capture by Long Cylindrical Bodies Surrounded by Predominantly Scattering Media, AECL-462 (1959).
8. I.H. GIBSON; The Physics of LATREP, AECL-2548 (1966).
9. R.E. KAY and R.E. GREEN; Lattice Measurements with 7-Rod Clusters of Natural Uranium Carbide in Heavy Water Moderator Part 1: Neutron Density Fine Structures in a Lattice Cell AECL-2650 (1966) and Part 2: Neutron Spectrum Parameters in a Lattice Cell AECL-2651 (1966).

APPENDIX A

Detailed Neutron Density Measurements in a Lattice Cell;
28 Rod UO₂ Fuel, H₂O Coolant, 11" Square Lattice Pitch

This section summarizes the results obtained from neutron density fine structure measurements made in a cell of a lattice of 28 rod UO₂ fuel, cooled by room temperature light water, at a square pitch of 11".

The experimental techniques involved measurement of copper foil and manganese wire activities and correcting to relative total neutron densities using spectrum parameters measured using the In-Mn-Lu relative foil activity method. A detailed description for a similar set of experiments is given in Reference 9.

Table A1 lists values of total neutron density at various locations in a lattice cell relative to the fuel average total neutron density.

Figure A1 illustrates relative manganese wire activity distributions in three directions in the moderator; along a line between nearest neighbour fuel assemblies, designated West; along a line between fuel assemblies diagonally opposite in the square lattice, designated North-West, and along a cell boundary, designated North-South.

TABLE A1: RELATIVE TOTAL NEUTRON DENSITY MEASUREMENTS

n_{fuel}	n_{I}	n_{M}	n_{o}	n_{c}	n_{pt}
1.000 \pm .2%	0.663 \pm .3%	0.829 \pm .8%	1.170 \pm .4%	1.106 \pm .9%	1.785 \pm .9%

n_{a}	n_{ct}	n_{edge}	n_{corner}	n_{mod}
1.807 \pm .9%	1.819 \pm .9%	2.434 \pm .9%	2.650 \pm .3%	2.379 \pm .7%

fuel, I, M, o, c, pt, a, ct, mod, edge, corner refer to average values in the fuel, inner fuel rods, middle fuel rods, outer fuel rods, coolant, pressure tube, air gap, calandria tube and moderator, and point values at the cell edge and cell corner respectively, all relative to the fuel average.

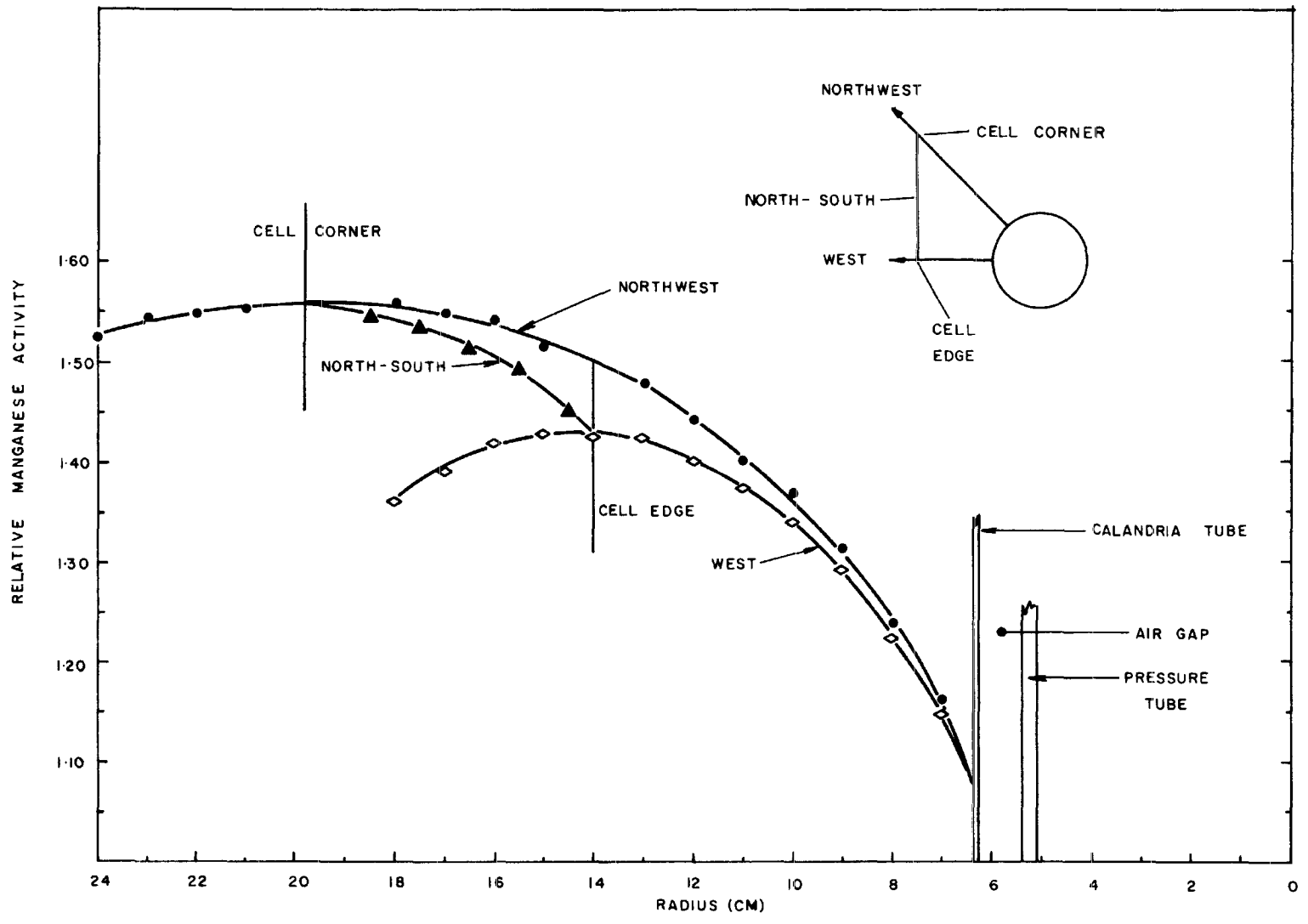


Fig. A1 Relative manganese activity distributions in moderator

APPENDIX B

Blackness Calculation of Neutron Density in ^{235}U Fuel

Measurements were made of relative total neutron density at the sheaths of the 18 fuel rods of the booster (see Sections III-2 and IV-2(b)). To predict the source production and absorption terms of equation (4), Section V, it is necessary to know the ratio of the neutron density at the sheath to the average neutron density in the fuel of a fuel rod; n_s/\bar{n}_{235} .

The ratio of the flux at the outside of a fuel rod to the average flux in the fuel was calculated for an infinitely long fuel rod in a predominantly scattering medium using Kushneriuk's expression⁽⁷⁾

$$G_{\text{app}} = \frac{\phi_s}{\phi_{\text{fuel}}} = \frac{a(2-\beta)}{\beta l_a}$$

where a is the radius of the absorber

l_a is the absorption mean free path in the fuel, and

β is the 'blackness' of the fuel.

Using appropriate values of 'a' and l_a , and tables of 'blackness' we obtain

$$G_{\text{app}} \approx \frac{n_s}{\bar{n}_{235}} = 1.18$$